Hydrodynamic Model for Gas-Lift Reactors

A. Eduardo Sáez, Marco A. Márquez, George W. Roberts, and Ruben G. Carbonell
Dept. of Chemical Engineering, North Carolina State University, Raleigh, NC 27695

The hydrodynamic model of Young et al. (1991) for external-loop gas-lift reactors was modified to account for buoyancy forces in the gas phase. The revised model is based on macroscopic balances for the gas-liquid separator and external downcomer and spatially-averaged, 1-D mass and momentum balances in the riser. Using only the physical properties of the gas and liquid phases, the reactor dimensions, and the gas superficial velocity, the model predicts gas holdup profiles, gas and liquid velocity profiles, and pressure profiles in the riser for bubbly flow. Empirical correlations are used to represent frictional and drag effects, but there are no adjustable parameters in the model. The system of equations that must be solved to predict hydrodynamic behavior is simpler than that of Young et al. The sensitivity of the model to choice of drag coefficient correlation is analyzed. The model predictions match experimental data of previous works.

Introduction

Modeling of gas-liquid and gas-liquid-solid reactors offers a number of advantages, including ease and reliability of reactor design and scale-up, and the ability to predict the effect of operating conditions. A comprehensive model of the reactor should include a description of the hydrodynamics, heat transfer, interfacial mass transfer, and reaction kinetics. The fundamental equations are a consequence of the principles of global and species mass conservation, thermal energy, and momentum. However, the formulation of a model from first principles is made difficult by the inherent geometrical complexity of a multiphase system, and by the fact that these processes typically involve turbulent flow.

A large number of hydrodynamic models have been developed for different types of multiphase reactors, including bubble columns (Fleischer et al., 1996; Zehner and Benfer, 1996; Sokolichin and Eigenberger, 1994; Romanainen and Salmi, 1991a, 1992), slurry bubble columns (Hillmer et al., 1994), stirred tanks (Romanainen and Salmi, 1991b, 1995; Haario and Seideman, 1994), and gas-lift reactors (Chisti et al., 1988; Young et al., 1991; Dluhy et al., 1994; Fleischer et al., 1996; Reinhold et al., 1996; Dhaouadi et al., 1996). Some of the models are based on drift-flux theory and macroscopic energy balances (Merchuk and Stein, 1981; Verlaan et al., 1986). Other models are based on mechanical energy balances and empirical correlations for the parameters that represent viscous dissipation effects (Chisti et al., 1988). Recent models have used the momentum equations to describe spatial variations of the hydrodynamic variables. Some of these models consider two-dimensional representations of velocity and gas holdup profiles (Sokolichin and Eigenberger, 1994), whereas others consider only axial variations of these parameters (Young et al., 1991; Hillmer et al., 1994).

In this work we will deal with external-loop gas-lift reactors (Figure 1). In these systems, gas and liquid flow upwards through the riser, where the chemical reaction takes place. The gas is disengaged from the liquid in the separation chamber, and liquid circulation is established through the downcomer. If the superficial gas velocity in the riser section is low enough, the flow pattern in the riser is bubbly flow, in which gas bubbles move uniformly upward, and there is negligible bubble dispersion with limited coalescence and breakup.

In principle, the hydrodynamics of a gas-lift reactor can be modeled from the fundamental equations of continuity and momentum by using spatially-averaged variables. Such an approach was followed by Young et al. (1991). That model was designed to predict the hydrodynamics of gas-liquid systems with bubbly flow in the riser under isothermal, nonreactive conditions. The model predicts axial variations of gas holdup and pressure, and it accurately describes experimental data for an air–water system. However, the model does not consider the effect of buoyancy forces in the gas and liquid momentum balances. The present work shows that taking buoyancy into account does not change the results significantly, but it simplifies the mathematical treatment and makes it more rigorous. As with the model of Young et al. (1991), the

Correspondence concerning this article should be addressed to G. W. Roberts.

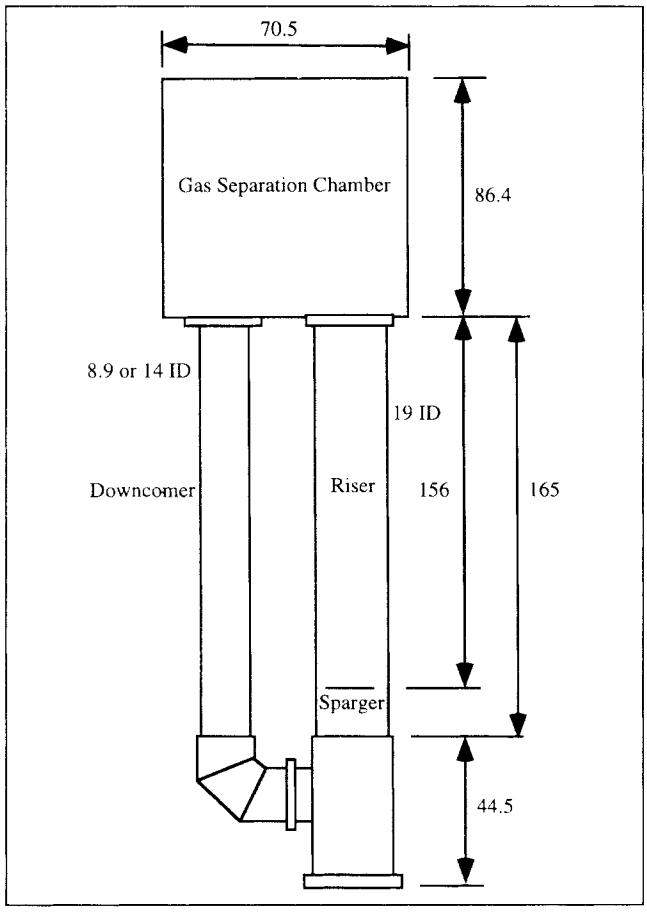

Figure 1. External loop airlift reactor used by Young et al. (1991).

Separator chamber is 27.9-cm wide; dimensions in cm.

new model is predictive and only requires empirical correlations to describe frictional effects and drag coefficients. An analysis of three different drag coefficient correlations has also been performed.

The use of a one-dimensional (1-D) model that predicts axial variations of holdup and pressure in the riser is especially useful when considering reactive systems in which appreciable amounts of gas phase are produced or consumed. In this case, there will be a strong coupling between the hydrodynamics, gas-liquid mass transfer, and reaction kinetics. A practical example of such an application is the reactive adsorption of CO_2 in aqueous NaOH or KOH when a gas phase that consists mostly of CO_2 is used (Amend, 1992; Fleischer et al., 1996). The reaction is so fast that gas-phase depletion is observed towards the top of the reactor. The model developed in the present work can be modified to account for chemical reactions and gas-liquid mass transfer so that it can be used as a part of a more complete simulation of a reactive system in a gas-lift reactor.

Model Formulation

The development of the model equations is presented. The equations for the riser are based on volume averages of the point equations of continuity and momentum after these have been time-averaged to account for turbulent flow. Under the assumption of bubbly flow, the equations lead to a 1-D model in the riser. The separator and downcomer are modeled by using the equations of continuity and macroscopic mechanical energy balances. The fundamental derivations have been presented by Young et al. (1991). The basic assumptions and equations obtained are summarized presenting detailed derivations only for the cases in which the present model departs from that developed by Young et al. All variables represent time-averaged quantities when turbulent flow is considered.

Riser

Continuity equations

Starting from the time-averaged point equation of continuity for each phase, Young et al. (1991) carry out an averaging process over a representative volume of gas-liquid suspension. The volume-averaged equations are then averaged over the cross-section of the riser. By assuming steady state, absence of chemical reaction, ideal gas, uniform liquid density, and negligible gas–liquid mass transfer, the following equations are obtained

$$\text{Liquid:} \quad \frac{d}{dz}\left[\rho_l(1-\bar{\epsilon})\langle\bar{v}_l\rangle\right]=0 \tag{1}$$

$$\text{Gas:} \quad \frac{d}{dz}\left[\bar{\rho}_g\bar{\epsilon}\langle\bar{v}_g\rangle\right]=0 \tag{2}$$

In these equations, the angular brackets represent intrinsic phase averages of the z-component of the phase velocities

$$\langle v_i\rangle=\frac{1}{V_i}\int_{V_i} v_i dV,\ i=g,l \tag{3}$$

where V_i is the portion of the averaging volume occupied by phase i, v_i is the point velocity of phase i, $(i=g,l)$, and g and l denote gas and liquid phases, respectively.

The bars in Eqs. 1 and 2 refer to cross-sectional averages, for example

$$\langle\bar{v}_i\rangle=\frac{1}{A}\int_A\langle v_i\rangle dA \tag{4}$$

where A is the cross-section of the riser.

The gas holdup is defined over the representative volume of gas-liquid suspension

$$\epsilon=\frac{V_g}{V_g+V_l} \tag{5}$$

In the development of Eqs. 1 and 2, terms that might give rise to dispersive contributions due to variations in the phase velocities throughout the cross-section have been neglected. These effects might be important in churn-turbulent flows where the liquid phase exhibits a strong recirculating motion within the riser. Therefore, this analysis is restricted to bubbly flows, for which dispersive contributions are small with respect to the mean flow.

Momentum equations

Young et al. (1991) start with the time-averaged point equations of motion

$$\rho_i\left(\frac{\partial \boldsymbol{v}_i}{\partial t}+\boldsymbol{v}_i\cdot\nabla\boldsymbol{v}_i\right)=-\nabla P_i+\rho_i\boldsymbol{g}+\nabla\cdot\tau_i^{(T)},\ i=g,l \quad (6)$$

where $\tau_i^{(T)}$ is the sum of the viscous and turbulent stress tensors.

In bubbly flow, the vertical component of the velocity vector of each phase dominates the horizontal component. Therefore, local inertial effects are negligible. By neglecting these terms and assuming steady state, the lefthand side of Eq. 6 is zero. By performing the volume average of the resulting equation, Young et al. arrive at the following equation for the liquid phase

$$-\nabla(1-\epsilon)\langle P_l\rangle+(1-\epsilon)\rho_l\boldsymbol{g}+\nabla\cdot(1-\epsilon)\langle\tau_l^{(T)}\rangle+\frac{1}{V}\int_{A_{gl}}(-P_l\boldsymbol{I}+\tau_l^{(T)})\cdot\boldsymbol{n}\,dA=0 \quad (7)$$

where $\langle P_l\rangle$ is the intrinsic phase average of the liquid pressure, A_{gl} is the area of gas-liquid interface within the averaging volume, $\boldsymbol{I}$ is the unit tensor, $\boldsymbol{n}$ is a unit vector normal to the gas-liquid interface (pointing into the gas phase), and $\langle\tau_l^{(T)}\rangle$ is the intrinsic phase average of the total stress tensor in the liquid phase.

The last term on the lefthand side of Eq. 7 represents the total force exerted at the gas-liquid interface. Young et al. interpreted this force as a drag force, thereby not considering the contribution of hydrostatic pressure variations to this term, which is the effect that leads to buoyancy forces, as shown below. In this work, we will express this term as proportional to the total interfacial force acting on the liquid per unit gas-liquid interfacial area $\boldsymbol{F}_t$,

$$a_{lg}\boldsymbol{F}_t=\frac{1}{V}\int_{A_{gl}}(-P_l\boldsymbol{I}+\tau_l^{(T)})\cdot\boldsymbol{n}\,dA \quad (8)$$

where a_{lg} is the gas-liquid interfacial area per unit volume of gas-liquid suspension.

The next step of the derivation is to take the axial component of Eq. 8 and average it over the cross-section of the riser. Young et al. showed that

$$\overline{[\nabla\cdot(1-\epsilon)\langle\tau_l^{(T)}\rangle]}_z=-\frac{f_r}{D}\frac{1}{2}\rho_l\langle\bar{v}_l\rangle^2 \quad (9)$$

where f_r is the friction factor at the wall of the riser, and D is the riser diameter. Equation 9 is based on the assumption that only the liquid phase interacts with the wall.

After assuming that terms involving cross-sectional averages of products of deviations with respect to averages (dispersive-like terms) are negligible with respect to products of averages, the procedure outlined by Young et al. leads to the following equation in the z-direction

$$-\frac{d}{dz}[\langle\bar{P}_l\rangle(1-\bar{\epsilon})]-(1-\bar{\epsilon})\rho_l g-\frac{f_r}{D}\frac{1}{2}\rho_l\langle\bar{v}_l\rangle^2+\bar{a}_{lg}\bar{F}_t=0 \quad (10)$$

The total vertical force per unit area at the gas-liquid interface can be expressed as the difference between downward drag and viscous forces per unit area ($\bar{F}_d$), and upward forces due to hydrostatic pressure variations per unit area ($\bar{F}_b$),

$$\bar{F}_t=\bar{F}_d-\bar{F}_b \quad (11)$$

To quantify $\bar{F}_b$, we will explore hydrostatic pressure effects at the gas-liquid interface in a control volume of length Δz in the riser, as depicted in Figure 2. From this representa-

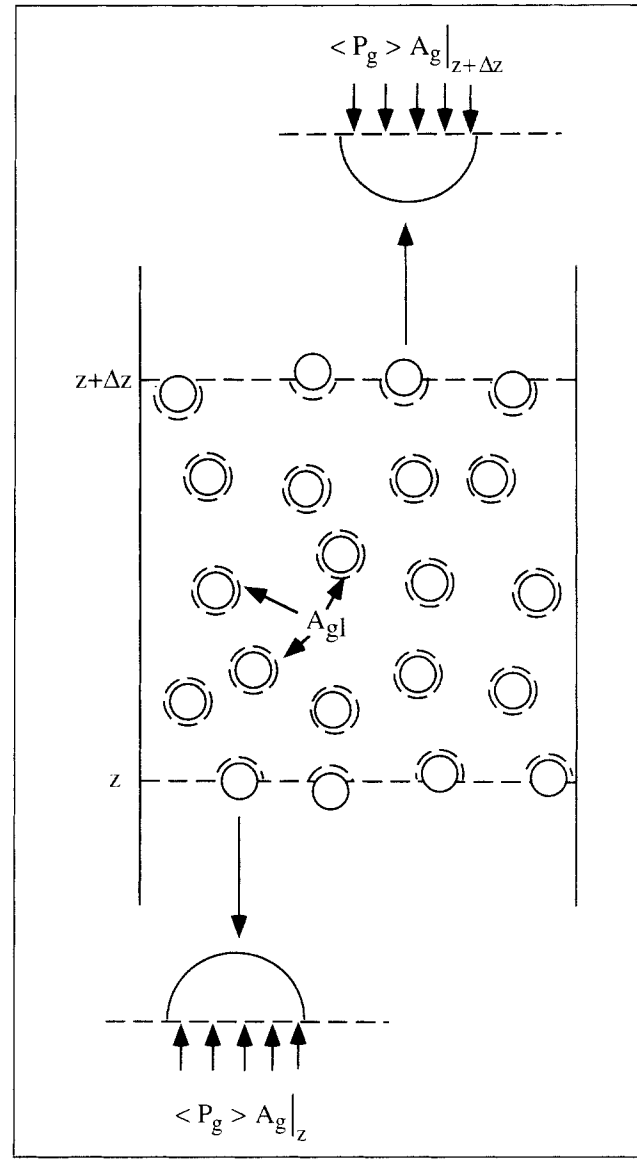

Figure 2. Control volume used to determine hydrostatic forces at the gas-liquid interface (dotted lines) in a section of riser.

tation, it can be seen that $\bar{F}_b$ corresponds to the total buoyancy force exerted on the bubbles contained in the control volume per unit gas-liquid interfacial area minus the external pressure forces exerted on the gas at the top and bottom sections of the control volume per unit gas-liquid interfacial area

$$\bar{F}_b = \frac{\bar{\epsilon}\rho_l g}{\bar{a}_{lg}} + \frac{\left(\langle \bar{P}_g \rangle A_g\right)|_{z+\Delta z} - \left(\langle \bar{P}_g \rangle A_g\right)|_z}{V\bar{a}_{lg}} \tag{12}$$

where in this case V is the control volume ($V = A\Delta z$). If we consider that $\bar{\epsilon} = A_g/A$, and take the limit as $\Delta z \to 0$, we obtain

$$\bar{F}_b = \frac{\bar{\epsilon}\rho_l g}{\bar{a}_{lg}} + \frac{1}{\bar{a}_{lg}} \frac{d\left(\langle \bar{P}_g \rangle \bar{\epsilon}\right)}{dz} \tag{13}$$

Pressure differences between gas and liquid phases can only be due to the pressure jump across the bubble surfaces due to surface tension effects. It can be shown that the pressure jump is appreciably lower than the values of gas and liquid pressures. Therefore, we will assume that liquid and gas pressures within an averaging volume are approximately the same. To a good degree of approximation we can then state

$$\langle \bar{P}_g \rangle = \langle \bar{P}_l \rangle = \langle \bar{P} \rangle \tag{14}$$

By using this fact, and Eqs. 10, 11, and 13, the liquid-phase momentum equation becomes

$$-\frac{d\langle \bar{P} \rangle}{dz} - \rho_l g - \frac{f_r}{D}\frac{1}{2}\rho_l \langle \bar{v}_l \rangle^2 + \bar{a}_{lg}\bar{F}_d = 0 \tag{15}$$

The friction factor f_r was determined from the empirical correlation developed by Akita et al. (1988) (see Young et al., 1991 for a discussion on the criteria that led to this choice)

$$f_r = \frac{0.187\sqrt{\bar{\epsilon}}}{(1-\bar{\epsilon})^{0.10}} \left(\frac{\sqrt{gD}}{\langle V_z \rangle}\right)^{1.1} \tag{16}$$

A similar approach can be followed for the gas-phase momentum equation. After applying the volume averaging technique to Eq. 6 for $i = g$, it is possible to show that the averaged gas-phase momentum equation can be written as follows

$$\frac{d(\bar{\epsilon}\langle \bar{P} \rangle)}{dz} - \bar{a}_{lg}\bar{F}_t = 0 \tag{17}$$

where gravitational effects have been neglected due to the relatively low density of the gas phase. Substitution of Eqs. 11 and 13 into Eq. 17 leads to

$$\bar{\epsilon}\rho_l g = \bar{a}_{lg}\bar{F}_d \tag{18}$$

This final form of the gas-phase momentum equation states that buoyancy balances the total drag and viscous forces at the gas-liquid interface. Therefore, the contribution of interfacial drag and viscous forces to the liquid momentum equation (Eq. 15) can be replaced by the buoyancy force, which yields

$$-\frac{d\langle \bar{P} \rangle}{dz} - (1-\bar{\epsilon})\rho_l g - \frac{f_r}{D}\frac{1}{2}\rho_l \langle \bar{v}_l \rangle^2 = 0 \tag{19}$$

This equation states that the pressure gradient in the liquid phase is due to hydrostatic contributions of the liquid holdup plus pressure losses due to wall friction.

Gas-Liquid Separator

Macroscopic mass balance

A macroscopic liquid mass balance in the gas-liquid separator states that the volumetric liquid flow rate leaving the riser should be equal to the volumetric liquid flow rate going into the downcomer

$$[(1-\bar{\epsilon})\langle \bar{v}_l \rangle]_{z=L} A = \bar{v}_{dc} A_{dc} \tag{20}$$

where $\bar{v}_{dc}$ is the cross-sectional area average of the liquid velocity in the downcomer, L is the length of the riser, and A_{dc} is the downcomer cross-sectional area. We have assumed that there is no gas in the downcomer.

Macroscopic mechanical energy balance

Young et al. (1991) performed a macroscopic mechanical energy balance in the separator, which was considered to be well mixed. Their analysis leads to the conclusion that the pressure at the top of the riser ($\langle \bar{P} \rangle_{z=L}$) and the pressure at the top of the downcomer are approximately equal. In addition, they assume that

$$\langle \bar{P} \rangle_{z=L} = P_a + \rho_l g h_t \tag{21}$$

which merely states that the pressure at the top of the riser is the same as that obtained under hydrostatic conditions. In Eq. 21, P_a is the atmospheric pressure, and h_t is the liquid level in the gas-liquid separator. Note that the gas holdup in the separator is considered to be very small. This equation can be used as a boundary condition for the integration of Eq. 19.

Downcomer

Macroscopic mechanical energy balance

To characterize the hydrodynamics of the downcomer, a macroscopic mechanical energy balance is performed in a control volume that extends from the top of the downcomer to the sparger in the riser. Young et al. (1991) present the details of the derivation. The final equation obtained has the following form

$$\left\{\left[\left(\frac{D_{dc}}{D}\right)^2-1\right]+f_{dc}\frac{L_{dc}}{D_{dc}}+\sum_i K_i\right\}\frac{\bar{v}_{dc}^2}{2g}+\frac{\langle\bar{P}\rangle_{z=0}-\bar{P}_{dc,z=L}}{\rho_l g}-L=0 \quad (22)$$

kinetic energy change (downcomer to riser) | wall friction | accessories | pressure contribution | gravitational contribution

In this equation, f_{dc} is the friction factor in the downcomer, D_{dc} is the downcomer diameter, and $\bar{P}_{dc,z=L}$ is the pressure at the top of the downcomer. The difference between the pressures at the top of the riser and the top of the downcomer due to kinetic energy changes and friction in the separator is neglected in the analysis, that is, $\bar{P}_{dc,z=L}=\langle\bar{P}\rangle_{z=L}$. The accessories term takes into account all mechanical energy losses in the control volume that are not due to wall friction. Young et al. (1991) include in this term losses in the elbow connecting the downcomer to the riser, and the expansion as the liquid enters the riser. In this work we will employ the same parameters used by Young et al. in their calculations in order to assess the effect of the more fundamental changes introduced into the riser momentum equations.

The friction factor f_{dc} to be used in Eq. 22 corresponds to the simple case of one phase flow, since we are assuming that there is no gas in the downcomer. This assumption is consistent with the observations of Young et al. during their experiments. Young et al. pointed out that the flow in the downcomer is developing flow. For this reason, they fitted these friction factors to their experimental data, obtaining values that varied with the L_{dc}/D_{dc} ratio: $f_{dc}=0.06$ for $L_{dc}/D_{dc}=14$, and $f_{dc}=0.04$ for $L_{dc}/D_{dc}=22$.

Gas-Liquid Drag and Viscous Forces

The gas-liquid drag and viscous forces per unit gas-liquid interfacial area ($\bar{F}_d$) will be determined from empirical correlations available in the literature. Young et al. (1991) present an analysis of the literature in the field. The drag force per unit area is expressed in terms of a drag coefficient $\hat{C}_d$ defined by

$$\bar{F}_d=\frac{1}{2}\hat{C}_d\rho_l\left(\langle\bar{v}_g\rangle-\langle\bar{v}_l\rangle\right)\left|\langle\bar{v}_g\rangle-\langle\bar{v}_l\rangle\right|\frac{A_p}{A_{gl}} \quad (23)$$

where A_p is the area of gas phase at a given cross-section. Note that the drag force is expressed as proportional to the square of the relative velocity between gas and liquid phases. If we assume that all the gas bubbles are perfect spheres, then $A_p=\Sigma_j\pi r_{bj}^2$ and $A_{gl}=\Sigma_j 4\pi r_{bj}^2$, where the sum includes all bubbles j in a given cross section. Equation 23 then simplifies to

$$\bar{F}_d=\frac{1}{8}\hat{C}_d\rho_l\left(\langle\bar{v}_g\rangle-\langle\bar{v}_l\rangle\right)\left|\langle\bar{v}_g\rangle-\langle\bar{v}_l\rangle\right| \quad (24)$$

The choice of correlation employed to calculate the drag coefficient might have a crucial impact in the results, considering that the gas-phase momentum equation (Eq. 18) directly relates buoyancy to gas-liquid drag and frictional effects. For this reason, we have analyzed the sensitivity of the model to the correlation employed.

Young et al. (1991) used exclusively the correlation developed by Ishii and Zuber (1979) for the case of monodisperse spherical bubbles of radius r_b

$$\hat{C}_d=\frac{4}{3}r_b\sqrt{\frac{g(\rho_l-\rho_g)}{\sigma(1-\epsilon)}} \quad (25)$$

where σ is the surface tension. We will refer to this correlation in the present work as Cd1.

According to Ishii and Zuber, Eq. 25 applies to distorted spherical bubbles with rigid interfaces that constitute what they refer to as the "distorted-bubble" regime. Its range of applicability is

$$N_\mu\geq 0.11\frac{(1+\Psi)}{\Psi^{8/3}} \quad (26)$$

where N_μ is the viscosity number, defined by

$$N_\mu=\frac{\mu_l}{\left[\rho_l\sigma\sqrt{\frac{\sigma}{g(\rho_l-\rho_g)}}\right]^{0.5}} \quad (27)$$

and

$$\Psi=0.55\left[(1+0.08R_b^3)^{4/7}-1\right]^{3/4} \quad (28)$$

where R_b is a dimensionless bubble radius, defined by

$$R_b=r_b\left[\frac{\rho_l g(\rho_l-\rho_g)}{\mu_l^2}\right]^{1/3} \quad (29)$$

The correlation of Ishii and Zuber gives a drag force per unit area, $\bar{F}_d$, that is directly proportional to the bubble radius. When this parameter is substituted into the gas-phase momentum equation (Eq. 18), the resulting equation is independent of bubble radius, since for monodisperse spherical bubbles

$$\bar{a}_{lg}=\frac{3\bar{\epsilon}}{r_b} \quad (30)$$

Therefore, when Cd1 is used, the model is independent of bubble size.

Two other correlations are considered in the present work as alternatives to Eq. 25. Both yield an explicit dependence of the gas-phase momentum equation on bubble size.

- Correlation Cd2 (Ishii and Zuber, 1979), valid for $Re < 2 \times 10^5$

$$\hat{C}_d = \frac{24}{Re}(1 + 0.1Re^{0.75}) \tag{31}$$

- Correlation Cd3 (Khan and Richardson, 1987), valid for $10^{-2} < Re < 3 \times 10^5$

$$\hat{C}_d = (2.25Re^{-0.31} + 0.36Re^{0.06})^{3.45} \tag{32}$$

where the Reynolds number is defined by

$$Re = \frac{\rho_l\left(\langle \bar{v}_g \rangle - \langle \bar{v}_l \rangle\right)2r_b}{\mu_l} \tag{33}$$

Correlations Cd2 and Cd3 consider the bubble as a solid particle moving through an infinite liquid at the slip velocity. Since bubble-bubble interactions are not taken into account, these correlations will be applicable for relatively low values of the gas holdup (ϵ). In addition, we have assumed a monodisperse size distribution for the bubbles.

Young et al. (1991) assumed that their external airlift configuration operating with an air-water system satisfied the criterion given by Eq. 26 at all of their operating conditions. In that case, the use of Cd1 is more convenient since the bubble size is absent from the formulation. However, in reacting systems where there is an appreciable decrease of bubble size as the reaction proceeds, the bubble radius might get to be low enough to make Cd1 invalid. For example, for the air-water system, the criterion given by Eq. 26 is not satisfied for bubble radii below about 1 mm. In this case, either Cd2 or Cd3 should give a better estimation of the drag coefficient.

When Cd2 or Cd3 are used in our formulation, it is necessary to know the bubble size as a function of position in the riser. In this case, the bubble radius at the sparger level ($z = 0$) must be measured or estimated. Presumably, this bubble radius (r_{b0}) will depend on the geometry of the distributor employed, the physical properties of the phases, and the gas and liquid velocities. Once r_{b0} is known, the value of r_b at any axial position can be estimated by assuming no bubble breakup or coalescence, which is reasonably valid for bubbly flow. Using the ideal gas equation, assuming an isothermal system, combined with the gas-phase continuity equation for the case of no mass transfer between gas and liquid yields

$$r_b = \left[\frac{\langle \bar{v}_g \rangle \bar{\epsilon}}{\left(\langle \bar{v}_g \rangle \bar{\epsilon}\right)_{z=0}}\right]^{1/3} r_{b0} \tag{34}$$

The case of a polydisperse bubble-size distribution can also be rigorously treated in a similar manner if the initial distribution at the sparger is known, as long as bubble interactions are neglected. However, in this work we will limit the application of the model to a monodisperse distribution.

Model Implementation

In this section we will describe the procedure employed in solving the model previously described. The basic information that must be available consists of: the riser and downcomer lengths L and L_{dc}, the riser and downcomer diameters D and D_{dc}, physical properties of the fluids (ρ_l, ρ_g, μ_l, σ), atmospheric pressure P_a, operating temperature T, the liquid level in the gas-liquid separator h_l, the bubble radius at the sparger r_{b0} ($z = 0$) (only when Cd2 or Cd3 are employed), and the gas superficial mass velocity (gas mass-flow rate per unit cross-sectional area) L_g.

Integrating the liquid-phase continuity equation (Eq. 1) yields

$$\rho_l(1 - \bar{\epsilon})\langle \bar{v}_l \rangle = L_f \tag{35}$$

where L_f is the superficial mass velocity of the liquid phase (liquid mass-flow rate per unit cross-sectional area), whose value is independent of axial position. This value represents the mass of liquid per unit time and unit riser area that is circulating through the system, which is not known *a priori*. The solution procedure starts by assuming a value for L_f.

Integrating the gas-phase continuity equation (Eq. 2) after using the ideal gas equation yields

$$\frac{\langle \bar{P} \rangle M_g}{RT}\bar{\epsilon}\langle \bar{v}_g \rangle = L_g \tag{36}$$

where L_g is the superficial mass velocity of the gas phase, which is also independent of axial position.

The pressure at the top of the riser is calculated from Eq. 21. Once L_f is known, the gas-phase momentum equation (Eq. 18) combined with the appropriate drag coefficient correlation, along with Eqs. 35 and 36 evaluated at the top of the riser ($z = L$) represent a system of three nonlinear algebraic equations with three unknowns: the gas and liquid velocities, and the gas holdup. These equations are solved and the results constitute a starting point for the integration of the liquid-phase momentum equation (Eq. 19), when correlation Cd1 is used. This differential equation was discretized by a Runge-Kutta algorithm, and solved by following a step-by-step procedure from the top of the riser. In each step, once the pressure is calculated from the Runge-Kutta discretization, Eqs. 18, 35, and 36 are solved to yield the local values of liquid and gas velocities and gas holdup.

When correlations Cd2 or Cd3 are used, the value of the initial bubble radius is specified and the average pressure at $z = 0$ is assumed. The liquid-phase momentum equation (Eq. 19) is then integrated from the bottom of the riser, the local bubble radius at each height is found by Eq. 34, and the local values of cross-sectional averages of the liquid and gas velocities and the gas holdup are once again calculated by solving Eqs. 18, 35, and 36 simultaneously. When the calculation reaches the top of the riser, the calculated average pressure at $z = L$ is compared with the known value. If these values do not coincide, a new average pressure at the bottom of the riser is assumed and the integration procedure is repeated.

Once the pressure, velocities, and gas holdup at the sparger are known, the mechanical energy balance in the downcomer

(Eq. 22) is used to calculate $\bar{v}_{dc}$. A new value of L_f is then found by combining Eqs. 20 and 35. If this value is different from the one used in the previous iteration, a new value for L_f is assigned and the iteration procedure continues. When the procedure converges, the solution gives the pressure, phase velocities, gas holdup, and bubble radius profiles in the riser (bubble radii are not calculated when Cd1 is employed).

It is interesting to point out that this model does not require the specification of a boundary condition for the gas holdup, since the only differential equation (Eq. 19) has the average pressure as a dependent variable, for which Eq. 21 acts as the only necessary boundary condition. Young et al.'s model required an additional boundary condition for the gas holdup, which was taken as a zero derivative condition at the top of the riser. This condition is not required by the present model, and is inappropriate for many situations involving chemical reaction and/or gas-liquid mass transfer.

Results and Discussion

The results obtained with the new model were compared with experimental data from Young et al. (1991), Merchuk and Stein (1981), Ghirardini et al. (1992), and with predictions obtained by applying the original model of Young et al. (1991). For both the present and Young et al.'s models, the drag coefficient correlation Cd1 was used. Figures 3 and 4 show the gas holdup as a function of axial position for two different downcomer diameters. Each figure contains the results for four different gas superficial velocities. The predictions of both models are very similar, except that the new model predicts a slightly stronger dependence of the gas holdup with axial position. In essence, axial variations of gas holdup in these cases are due to the decrease in hydrostatic pressure with height. The axial variation of gas holdup becomes more pronounced as the superficial gas velocity increases because of the higher void fraction in the column. For taller, production-scale reactors, the axial variation in the void fraction due to the hydrostatic effect could be substantial, and the new model should predict this trend more accurately.

The absolute error of the two models with respect to experimental data for the other hydrodynamic variables, that is,

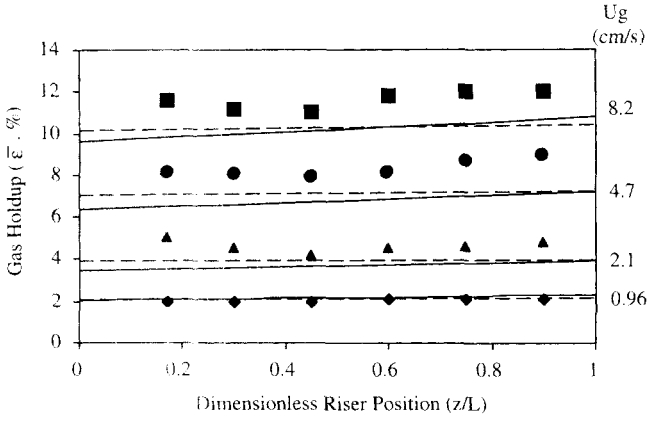

Figure 3. Gas holdup profiles, downcomer diameter: 0.14 m.

Solid lines: present model; dashed lines: Young et al.'s model; data points: Young et al. (1991) (D = 0.19 m; L = 1.56 m).

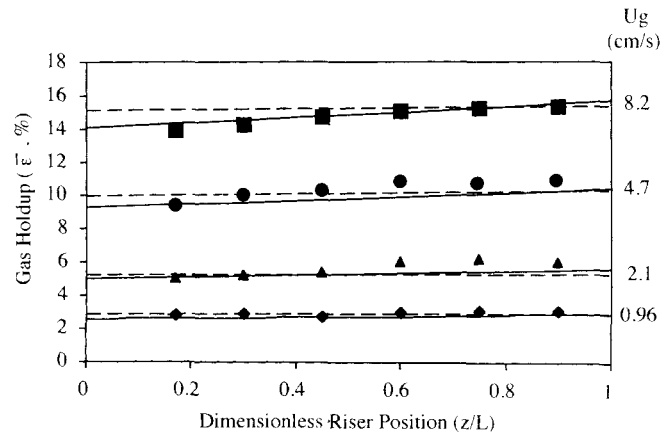

Figure 4. Gas holdup profiles, downcomer diameter: 0.089 m.

Solid lines: present model; dashed lines: Young et al.'s model; data points: Young et al. (1991) (D = 0.19 m; L = 1.56 m).

pressure, actual riser gas and liquid velocities, and liquid circulation rate, was similar. Since small differences in the pressure can have a large effect on the liquid circulation rate, the pressure at the sparger must be predicted within a very close tolerance. With both models, the difference was less than 1% in most cases. For the rest of the hydrodynamic variables, the relative deviation with respect to experimental data ranged from 0 to 22% in magnitude with both models. These values are close to the errors in mass balance closure calculated by Young et al. (1991).

Chisti et al. (1988) developed a simplified correlation to predict liquid circulation rate and average gas holdups in gas-lift reactors by performing a macroscopic mechanical energy balance that neglects axial variations in phase velocities and gas holdup in the riser. Their equation can be used to calculate the superficial liquid velocity in the riser as a function of the gas-liquid dispersion height, reactor dimensions, riser and downcomer gas holdup, and empirical frictional coefficients. This correlation predicts the superficial liquid velocity and the void fraction in the riser simultaneously using an iterative procedure. This model is potentially useful for reactors in which there is no coupling between mass transfer or reaction with the hydrodynamics. Figures 5 and 6 present a comparison of the experimental data from Young et al. (1991) with the predictions given by the original model of Young et al., the model developed in this work, and the correlation of Chisti et al.

Figure 5 shows the variation of the global gas holdup in the riser with superficial gas velocity, and Figure 6 presents the results for liquid circulation flux. For the present model and the model of Young et al., the global gas holdup (ϵ_g) in the riser was calculated by

$$\epsilon_g = \frac{1}{L}\int_0^L \bar{\epsilon}\, dz \tag{37}$$

The experimental values of the global gas holdup, presented in Figure 5, agree reasonably well with all three models, but the present model gives the most accurate prediction.

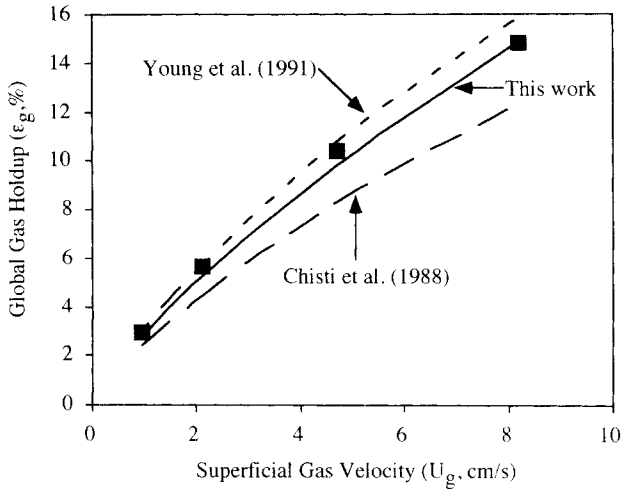

Figure 5. Global gas holdup as a function of gas superficial velocity.

Downcomer diameter: 0.089 m. Data points: Young et al. (1991).

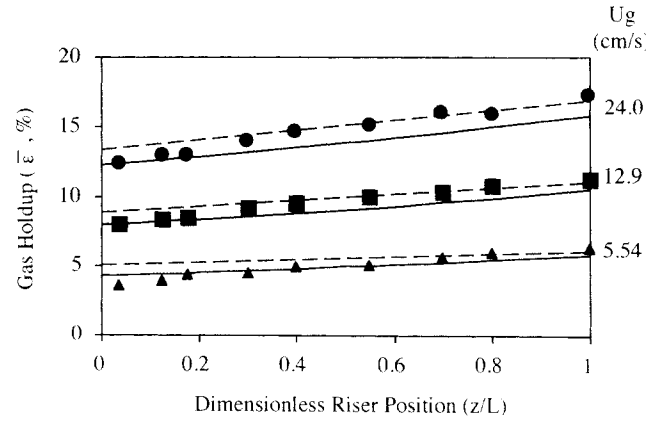

Figure 7. Gas holdup profiles.

Downcomer diameter: 0.14 m. Solid lines: present model; dashed lines: Young et al.'s model; data points: Merchuk and Stein (1981) (D = 0.14 m; L = 4.05 m).

Chisti et al.'s correlation underestimates the gas holdup. The experimental values of the liquid circulation flux, presented in Figure 6, agree well with the predictions of the present model and Young et al.'s model, but Chisti et al.'s correlation severely underestimates liquid circulation.

Predictions from the new model were also compared with the experimental data of Merchuk and Stein (1981). These data were obtained with a riser that was appreciably taller than that used by Young et al. which suggests a larger variation in hydrostatic pressure in the riser, and a larger effect of the wall friction term in the macroscopic mechanical energy balance in the downcomer. For comparison purposes, frictional losses in the accessories were estimated to be the same as those corresponding to Young et al.'s calculations. Merchuk and Stein also employed appreciably higher superficial gas velocities, thus providing a quite different set of operating conditions from Young et al.'s experiments. Figure 7 shows that gas holdup profiles in the riser are accurately predicted by the present model, as well as by Young et al.'s model. Relative variations of gas holdup are larger in this case, as expected.

Global gas holdup and liquid circulation flux measurements are shown as a function of the superficial gas velocity in Figures 8 and 9, respectively. The results show that Young et al.'s model describes the global gas holdup very well over the whole range of gas superficial velocity. The present model underpredicts the gas holdup by about 1% in absolute terms, and the correlation of Chisti et al. underpredicts those values to an even greater extent. Although Chisti et al.'s correlation gives a better prediction of liquid circulation flux than the present model (Figure 9), the latter is always within 20% of the experimental values.

Finally, we have compared the present model with experimental data obtained by Ghirardini et al. (1992), who worked

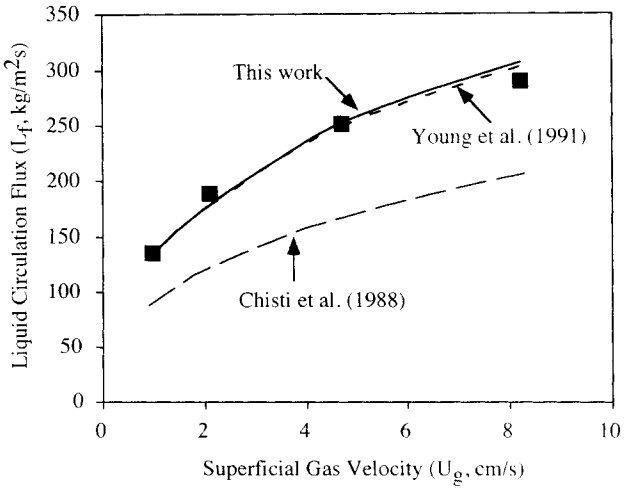

Figure 6. Liquid circulation flux as a function of gas superficial velocity.

Downcomer diameter: 0.089 m. Data points: Young et al. (1991).

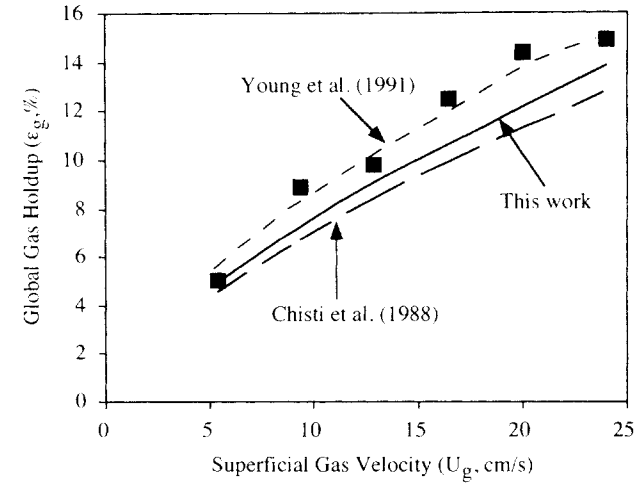

Figure 8. Global gas holdup as a function of gas superficial velocity.

Data points: Merchuk and Stein (1981).

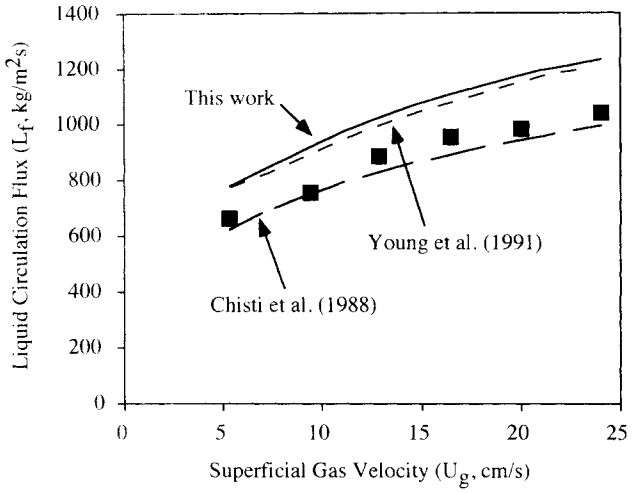

Figure 9. Liquid circulation flux as a function of gas superficial velocity.

Data points: Merchuk and Stein (1981).

with very high superficial gas velocities. The actual riser liquid velocities are shown in Figure 10 as a function of gas superficial velocity. The model overpredicts the data by about 20%. Due to the lack of detail of the experimental setup, we have employed the same accessories losses as in Young et al.'s calculations. Considering this uncertainty and the high values of both gas and liquid velocities, the prediction can be considered adequate. Furthermore, Ghirardini et al. report that there was gas in the downcomer in some of the experiments, which would tend to decrease liquid circulation. Global gas holdups in the riser predicted by the model were not compared to experimental values, since Ghirardini et al. do not provide information on this parameter.

The results presented in this section show that the new mathematical model is capable of predicting accurately the hydrodynamic parameters of a gas-lift reactor, including gas holdup profiles in the riser section, and liquid circulation velocities.

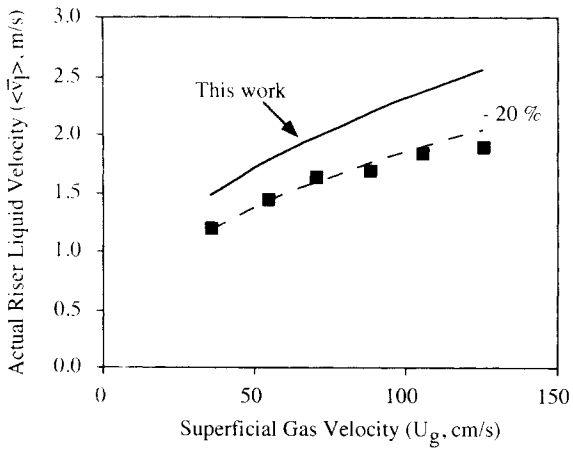

Figure 10. Actual riser liquid velocity as a function of gas superficial velocity.

Data points: Ghirardini et al. (1992) ($D = D_{dc} = 0.10$ m, $L = 2$ m). The calculated values were evaluated at $z/L = 0.5$.

Drag Coefficient Analysis

The predictions of the present model depend on the empirical correlation selected to calculate gas-liquid drag and frictional effects. In this section we explore the sensitivity of the model to the choice of drag coefficient correlation by comparing results at the same operating conditions when correlations Cd1, Cd2, and Cd3 are employed.

Figure 11 shows the axial change in gas holdup predicted by the new model using different drag coefficient correlations and different initial bubble radii. The results have been compared to the experimental data of Young et al. (1991). As noted previously, the predicted values with correlation Cd1 are independent of bubble size. For correlations Cd2 and Cd3, the prediction changes significantly with bubble radius. Correlations Cd2 and Cd3 predict very similar results for a given bubble radius, since they both represent the drag coefficient for flow around a rigid sphere. With these two correlations, larger bubbles rise at a higher velocity and, consequently, the gas holdup decreases as the bubble size increases. This trend is apparent in the results shown in Figure 11.

All three correlations give similar results when r_{b0} is 1 mm. This suggests that this bubble size might be close to the real bubble size at the sparger attained in the experiments. The values obtained with Cd2 and Cd3 for $r_{b0} = 2.5$ mm are within 10% of each other and the difference becomes smaller as r_{b0} decreases, as observed for $r_{b0} = 0.5$ mm, for which the results for Cd2 and Cd3 are within 1%.

Figures 12 and 13 present the average gas holdup and the liquid circulation flux for different gas superficial velocities and different initial bubble radii. The results follow the same trend observed in the gas holdup profiles: for the initial bubble radius of 1 mm, the three correlations practically coincide and all accurately represent the experimental data.

It is evident from the results that the use of correlations Cd2 and Cd3 require an accurate knowledge of the bubble radius. On the other hand, the explicit dependence on initial bubble radius disappears when the Cd1 correlation is used.

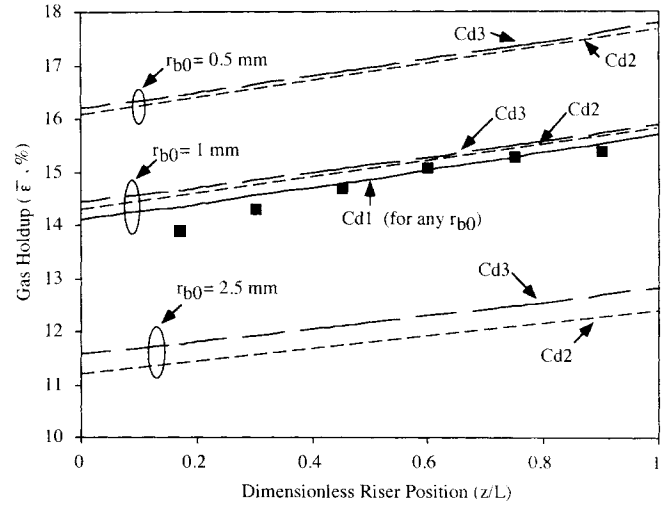

Figure 11. Effect of bubble size at the sparger on gas holdup profiles for various drag coefficient correlations.

Data points: Young et al. (1991); $D_{dc} = 0.089$ m; $U_g = 8.2$ cm/s.

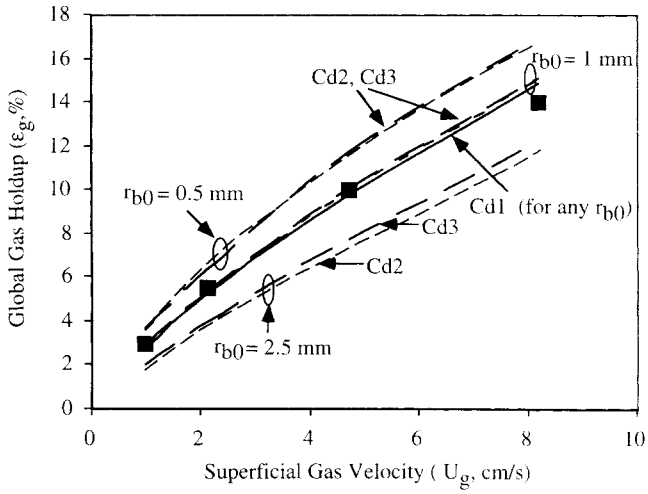

Figure 12. Effect of bubble size at the sparger on global gas holdup for various drag coefficient correlations.

Data points: Young et al. (1991); D_{dc} = 0.089 m.

However, an implicit dependence remains since this correlation is valid only for a certain range of bubble sizes in the distorted particle regime (Ishii and Zuber, 1979). Correlation Cd1 effectively predicts the data from Young et al. (1991) and Merchuk and Stein (1981). If the initial bubble radius were 1 mm, correlation Cd1 would satisfy the criterion given by Eq. 26.

It is part of a future work to extend the present model to reacting systems where there is a substantial change in the bubble size as the reaction proceeds, that is, the gas bubbles expand or contract. In this case, a combination of drag coefficient correlations might be required in order to handle the varying bubble size, and a knowledge of the initial bubble radius will be required. In addition, the assumption of complete gas disengagement in the gas-liquid separator may not be appropriate for very small bubble radii.

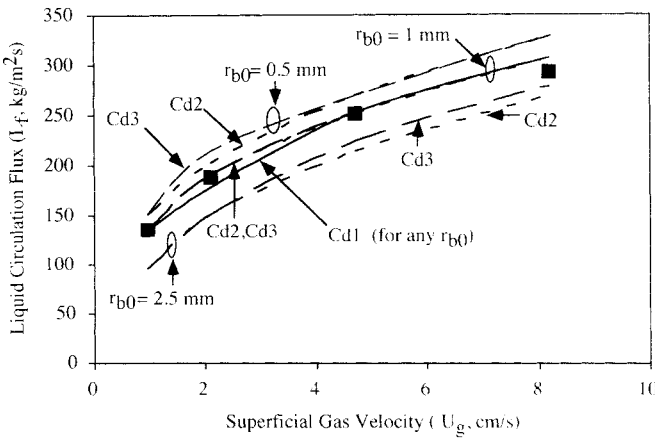

Figure 13. Effect of bubble size at the sparger on liquid circulation flux for various drag coefficient correlations.

Data points: Young et al. (1991); D_{dc} = 0.089 m.

Conclusions

A model to describe gas-lift reactor hydrodynamics has been developed by revising the formulation of Young et al. (1991) to include buoyancy effects in the momentum balances in the riser. The main advantage of the new model is that its simulation of the riser requires the solution of only one differential equation, the liquid-phase momentum equation. This eliminates the need for a boundary condition for the gas holdup, which is very difficult to formulate on physical grounds. The new model accurately predicts experimental data from several sources that span a wide range of gas superficial velocities, and riser and downcomer dimensions. Three different drag coefficient correlations were tested in the representation of gas-liquid drag and frictional effects. When the drag coefficient is an explicit function of the Reynolds number, a knowledge of the bubble size at the sparger is required to determine the pressure, gas holdup and phase velocity profiles in the riser. The model is sensitive to the value of that initial bubble size.

Notation

A_g = cross-sectional area of riser occupied by gas phase
g = acceleration of gravity
M = molecular weight
U_g = gas superficial velocity, based on riser cross section and atmospheric pressure
$\langle x \rangle$ = denotes volume average of x, defined by Eq. 3
$\bar{x}$ = denotes cross-sectional average of x in the riser, defined by Eq. 4
z = axial coordinate

Literature Cited

Akita, K., T. Okazaki, and H. Koyama, "Gas Holdup and Friction Factors of Gas-Liquid Two Phase Flow in Air-Lift Bubble Column," *J. Chem. Eng. Jpn.*, **21**, 476 (1988).

Amend, R. J., "Effect of Chemical Reactions on the Hydrodynamics of an Airlift Reactor," M.Sc. Thesis, Dept. of Chemical Engineering, North Carolina State University (1992).

Chisti, Y., B. Halard, and M. Moo-Young, "Liquid Circulation in Airlift Reactors," *Chem. Eng. Sci.*, **43**, 451 (1988).

Dhaouadi, H., S. Poncin, J. M. Hornut, G. Wild, and P. Oinas, "Hydrodynamics of an Airlift Reactor: Experiments and Modelling," *Chem. Eng. Sci.*, **51**, 2625 (1996).

Dluhy, M., J. Sefcik, and V. Bales, "Mathematical Modelling of Air-Lift Bioreactor for Waste Water Treatment," *Chem. Eng. Sci.*, **18**, S725 (1994).

Fleischer, C., S. Becker, and G. Eigenberger, "Detailed Modeling of the Chemisorption of CO_2 into NaOH in a Bubble Column," *Chem. Eng. Sci.*, **51**, 1715 (1996).

Ghirardini, M., G. Donati, and F. Rivetti, "Gas Lift Reactors: Hydrodynamics, Mass Transfer, and Scale Up," *Chem. Eng. Sci.*, **47**, 2209 (1992).

Haario, H., and T. Seideman, "Reaction and Diffusion at a Gas/Liquid Interface," *SIAM J. Math. Anal.*, **25**, 1069 (1994).

Hillmer, G., L. Weismantel, and H. Hofmann, "Investigations and Modelling of Slurry Bubble Columns," *Chem. Eng. Sci.*, **49**, 837 (1994).

Ishii, M., and N. Zuber, "Drag Coefficient and Relative Velocity in Bubbly, Droplet or Particulate Flows," *AIChE J.*, **25**, 843 (1979).

Khan, A. R., and J. F. Richardson, "The Resistance to Motion of a Solid Sphere and a Fluid, *Chem. Eng. Comm.*, **62**, 135 (1987).

Merchuk, J. C., and Y. Stein, "Local Hold-up and Actual Liquid Velocity in Air-Lift Reactors," *AIChE J.*, **27**, 377 (1981).

Reinhold, G., S. Merrath, F. Lennemann, and H. Märkl, "Modelling the Hydrodynamics and the Liquid-Mixing Behavior of a Biogas Tower Reactor," *Chem. Eng. Sci.*, **51**, 4065 (1996).

Romanainen, J. J., and T. Salmi, "Numerical Strategies in Solving Gas-Liquid Reaction Models-1. Stagnant Films and a Steady State CSTR," *Comp. Chem. Eng.*, **15**, 763 (1991a).

Romanainen, J. J., and T. Salmi, "Numerical Strategies in Solving Gas-Liquid Reaction Models-2. Transient Film and Dynamic Tank Reactors," *Comp. Chem. Eng.*, **15**, 783 (1991b).

Romanainen, J. J., and T. Salmi, "The Effect of Reaction Kinetics, Mass Transfer and Flow Pattern on Non-Catalytic and Homogeneously Catalyzed Gas-Liquid Reactions in Bubble Columns," *Chem. Eng. Sci.*, **47**, 2493 (1992).

Romanainen, J. J., and T. Salmi, "Numerical Strategies in Solving Gas-Liquid Reaction Models-3. Steady State Bubble Columns," *Comp. Chem. Eng.*, **19**, 139 (1995).

Sokolichin, A., and G. Eigenberger, "Gas-Liquid Flow in Bubble Columns and Loop Reactors: Part I. Detailed Modelling and Numerical Simulation," *Chem. Eng. Sci.*, **49**, 5735 (1994).

Verlaan, P., J. Tramper, and K. Van't Reit, "A Hydrodynamic Model for an Airlift Loop Bioreactor with External Loop," *Chem. Eng. J.*, **33**, B43 (1986).

Young, M. A., R. G. Carbonell, and D. F. Ollis, "Airlift Bioreactor: Analysis of Local Two-Phase Hydrodynamics," *AIChE J.*, **37**, 403 (1991).

Zehner, P., and R. Benfer, "Modeling Fluid Dynamics in Multiphase Reactors," *Chem. Eng. Sci.*, **51**, 1744 (1996).

Manuscript received Dec. 12, 1997, and revision received Mar. 12, 1998.